EUROfusion

WPMAG-CPR(18) 20020

I Tiseanu et al.

Multi-scale 3D modelling of a DEMO prototype cable from strand to full-size conductor based on X-ray tomography and image analysis

Preprint of Paper to be submitted for publication in Proceeding of
30th Symposium on Fusion Technology (SOFT)

This work has been carried out within the framework of the EUROfusion Consortium and has received funding from the Euratom research and training programme 2014-2018 under grant agreement No 633053. The views and opinions expressed herein do not necessarily reflect those of the European Commission.

Multi-scale 3D modelling of a DEMO prototype cable from strand to full-size conductor based on X-ray tomography and image analysis

Ion Tiseanu[a], Luigi Muzzi[b], Adrian Sima[a], Daniel Dumitru[a], Cosmin Dobrea[a], Teddy Craciunescu[a], Mihail Lungu[a], Ioana Porosnicu[a], Valentina Corato[b], Antonio della Corte[b]

[a]*National Institute for Lasers, Plasma and Radiation Physics (INFLPR), Magurele-Bucharest, Romania*
[b]*Superconductivity Laboratory, ENEA, Frascati, Italy*

The design of a superconducting magnet system of a fusion reactor candidate is usually based on the Cable in Conduit Conductor (CICC) concept. CICC consist of complex structures with several hundreds of highly packed, multistage twisted superconductor and copper strands, cooling structures – all wrapped in thin steel foils and jacketed in relatively thick stainless-steel pipes. As recently demonstrated, such complex morphology can be captured by fully 3D X-ray tomography. One of the three alternative winding pack (WP) options for the toroidal field coils of the European DEMO superconducting magnet system as proposed by the Italian ENEA, features a layer-wound WP design adopting a wind-and-react conductor with high aspect ratio rectangular cross section. A multi-physics modelling requiring high accuracy from the strand to the full-size conductor scale was tested on two X-ray tomography systems. For the microstructural integrity analysis of the internal tin one mm diameter Nb_3Sn strand, manufactured by Western Superconducting Technologies, a microtomograph with ~1 μm feature recognition was used. For the full-size conductor (66x25 mm^2 internal dimensions) a high energy (> 300 kVp) microtomograph with voxel resolution of ~20 μm was employed. Voids and/or geometrical imperfections were detected, accurately pin-pointed and locally investigated at high resolution before and after heat treatment. Dimensional measurements on the 3D internal structure of the strand showed the small dimensional changes of the strand after the heat treatment. A significant result was the determination of the twist-pitch factor in a purely non-invasive way. The 3D reconstructions of the CICC cables were used to verify the cabling and compaction processes as well as the structural integrity of the strands, wrapping foils and spiral cooling structures. Also, 3D reconstruction of strand trajectories provided a strong input for a multiphysical modelling/interpretation of mechanical–electrical properties of CICC in cryogenic–electromagnetic environments.

Keywords: X-ray tomography, Cable-in-Conduit, Nb_3Sn, strand trajectory, twist-pitch

1. Introduction

Prototype Nb_3Sn cable-in-conduit conductors (CICC) have been designed, manufactured and tested in the frame of the EUROfusion DEMO activities [1-3] with the goal to operate the high performance conductors at higher fields than ITER toroidal field (TF) conductors, enabling the construction of low cost, compact, high field tokamaks [4].

One of the three alternative winding pack (WP) options, as proposed by ENEA, the DEMO Wind&React (W&R) rectangular CICC is characterized by the presence of small, distributed pressure relief channels. In the evaluation of the thermo-hydraulic performance [5] of the conductor, especially in case of quench [6], it is essential to consider all possible paths for the helium inside the CICC cross-section. What is often observed on 2D cross-section analysis is that some local voids are present on the inner corners, due to the fact that the rectangular geometry is obtained by compaction starting from a round cable inserted inside a round steel tube. A 3D characterization of such voids results of fundamental importance, to understand whether these channels extend continuously longitudinally, and can thus be considered free channels for the supercritical helium circulation inside the CICC, in parallel to the pressure relief channels and the cable bundle.

Additionally, the present CICC is characterized by a relatively low local void fraction, inside the cable bundle (of about 27%-28%). Due to this, and to the change of geometry during compaction (from round to rectangular), it is important to analyze possible strand deformations or damages at the strand level.

On the other hand, the complex trajectories of the strands interleaved in the conductor cable volume cannot be easily predicted while having an influence on both hydraulic and electromagnetic performances. The electric critical properties will be impacted by the statistics of strand angles with respect to the magnetic field together with the statistics of strand performances along production.

As recently demonstrated, such complex morphology can be captured by fully 3D X-ray tomography (XCT), [7-9]. The technique of 3D X-ray microstructure characterization is, to this aim, a powerful analysis technique, that might reveal important information, as advanced 3D modeling of strands geometry and void homogeneity, and provide guidelines for the CICC design.

In [8] the Nb_3Sn strand bending in the ITER TF cable at the He-inlet was investigated at ~0.1 mm maximum resolution. Accurate non-destructive examinations of JT-

author's email:ion.tiseanu@inflpr.ro

60SA TF conductor were both developed by INFLPR laboratory and gradually improved [7,9] so as to allow routine examination on a large number of batches, with a good accuracy at the strand dimensions level.

Few studies conducted with laboratory [10-12] and synchrotron [13, 14] X-ray microtomography were concerned with 3D modelling of multifilamentary superconductor strands. Visualization of the details of the architecture of wires with different topologies, inspection of the geometrical perfection of the component elements and, especially, the non-invasive determination of the twist-pitch factor of Nb_3Sn and MgB_2 strands were the main results of [10, 11]. Comisso et. al. [12] use successive tomographic scans to analyze the contact interaction between Nb_3Sn superconductor and copper strands in an older CICC cable by determining the void fraction, twist pitch factor and the trajectory of the Nb_3Sn strands. High resolution analysis on Nb_3Sn strand matrix are performed by synchrotron radiation computed tomography [13, 14], where the aim of the studies was the identification and characterization of possible void formation.

2. Tomography Equipment and Methods

Current development of the laboratory X-ray tomography equipment allow us to conduct a multiscale analysis from Nb_3Sn strand to full scale cable for one of the advanced CICC DEMO prototype conductor.

Volumetric analysis at individual and multiplet strand level is possible at our high resolution tomograph based on a transmission nanofocus X-ray source and a high digital output, 2Kx2K X-ray detection array. Special care is addressed to obtain sharpest focus spot (~ 1 µm) with the help of a JIMA Micro Resolution Chart for X-Ray. The thermal stability of the focus is maintained with additional X-ray tube cooling.

High-resolution images for full scale CCIC samples jacketed in rectangular stainless steel pipes are obtained by a combination of high energy / intensity and small focus spot X-ray source and high resolution /efficiency detector array.

To assess the capability of the XCT method to deliver relevant inspection of the full cross-section ENEA CICC (66x25 mm interior dimensions) two configurations were evaluated:

1. Maximum 300 kV microfocus monopolar X-ray source with typical focus spot of couple of tens of µm.
2. Maximum 450 kV bipolar X-ray source with focus spot ~100 µm.

Both XCT systems were fitted with state-of-the-art large flat panel X-ray detection arrays.

Numerical modelling and experimental activities were performed for the optimization of the two X-ray computer tomography systems for CICC TF conductors and joints. Numerical modelling consisted of Monte Carlo simulation (PENELOPE2014 code) of the X-ray generation and transport in the tomographic configurations. The superconductor/resistive joint were analyzed for the two different (XCT) configurations with respect to delivered X-ray energy.

The simulations were realized in two steps:

In the first step the X-ray spectra was simulated for a tungsten target hit by electron beam of 300 and 450 keV in the conventional reflection geometry, detecting thus the Bremsstrahlung spectrum into a Be window of 0.5 mm thickness.

Secondly, the X-ray spectra is transported and detected in the XCT configuration that modeled different types of defects such as voids or pinched/deformed strands. The numerical modelling was optimized in order to analyze a complex part of TF DEMO cable/joint which is the most difficult to penetrate by X-rays, considering that the results can also be applied to less complicated structure of TF joints.

As a result, comparing all the simulations, we observed that for both tomography configurations (300 kV and 450 kV) we are able to identify the type of the defect based on the signal intensity. Furthermore, we have also analyzed the effect of the jacket thickness to the signal intensity.

These simulation results were methodically verified by experiments as will be shown in the next sections.

3. Results and discussion

3.1 Cable level

Structural integrity analysis

Sections of ~150 mm of ENEA prototype cable were scanned by two tomographs: one with a microfocus X-ray source operated at ~300 kV and the other with a bipolar X-ray tube operated at ~400 kV.

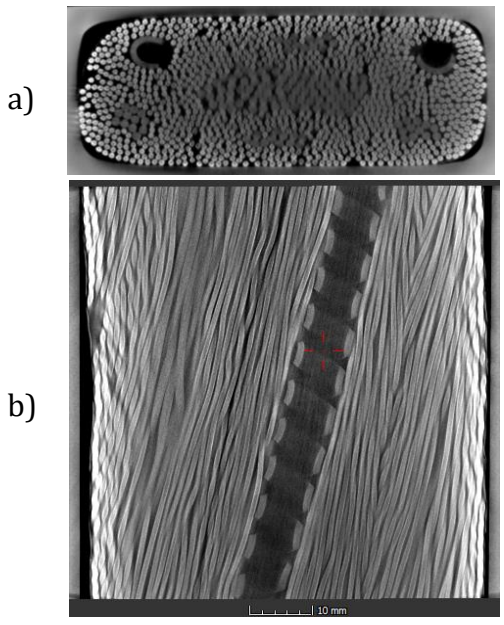

Fig. 1. a) Transversal (scanned at ~400kV, ~50 µm per voxel) and b) axial (scanned at ~300 kV, ~15 µm per voxel) tomography cross-sections of ENEA DEMO prototype conductor.

The reconstructed volumes are sampled at ~15 μm/voxel in the first case due to the high resolution detector array (4Kx4K, 100 μm/pixel). The voxel resolution of the >400 kV scan was ~50 μm/voxel due to a combination of larger focus spot and detector array pixel (2Kx2K, 200 μm/pixel).

Both measurements provided enough information for an accurate assessment with the microstructural integrity purpose. According to Fig. 1a) and b), the superconducting strands, copper wires, wrapping foils as well as the cooling structures are clearly visible. The cooling spirals don't show significant deformation. The six petal contours are discernible; the strand interaction regions with the cooling structures and copper wires are visible. The complex geometry of the wrapping foil (0.1 mm) and its structural integrity are clearly revealed.

Quantitative analysis

Emphasis is addressed to the 3D modeling of voids distribution and strands geometry. In general, only the high contrast/definition 400 kV scan images could be reliably processed towards quantifiable void and strand trajectory parameters. The significantly noisier 300 kV images, while usable for structural integrity assessment, offer only limited quantitative output.

Distribution of voids

The void fraction represents the ratio of the void and the interior area of the CICC sample. Void fraction evaluation is based on multiple thresholding of the gray level histogram of the tomographic volume (Fig. 2, top). The voids distribution is presented as pores color coded with the size/density. In our calculation, which was possible only for high contrast 400 kV images, the void fraction value was estimated as 0.30±0.02 which is agreement with nominal specification.

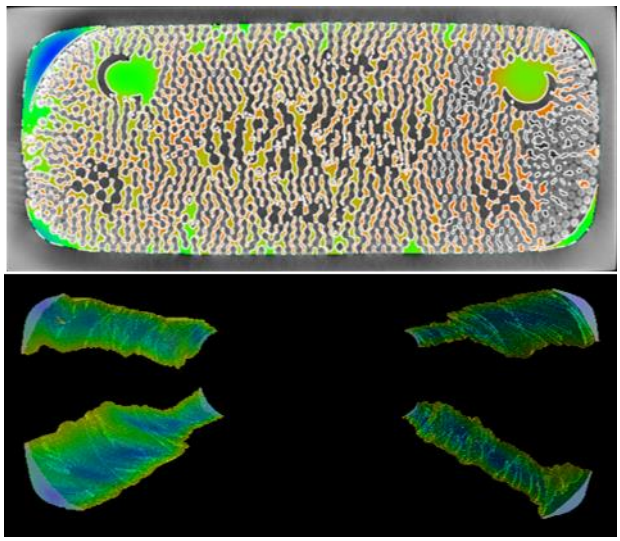

Fig. 2. Voids distribution in the ENEA CICC prototype: local distribution (top); corner voids (bottom).

Due to the change of geometry during compaction (from round to rectangular) it is important to assess the voids located in the corners. Inspection of ~30 cm of conductor shows that no corner "channel" is continuous over the whole length. Actually, each of the corner channels got at least one total strangulation on 30 cm of cable. From data shown in Fig 2 bottom, we could estimate corner voids volume at 40.3 cm^3 per 1 m of conductor.

Strands detection and trajectory reconstruction

In [6] and [8] we pursued different methods for the automatic strand detection and positioning followed by the application of a linear programming algorithm for connecting the strands in adjacent slices. The algorithm also allows optimization through the use of parameters, such as the maximum distance allowed between center of strand in adjacent slices and the number of slices a strand can miss on.

In the current work, due to dramatic improvement of the axial sampling resolution, an algorithm, based on a photometric analysis, was developed for combined strands detection and trajectory reconstruction. The main issue is to find real strand position when they are very close to each other and on a diffuse background. The strand image is modeled by a 2D Gaussian profile spread on a region typically of 10 x 10 pixels.

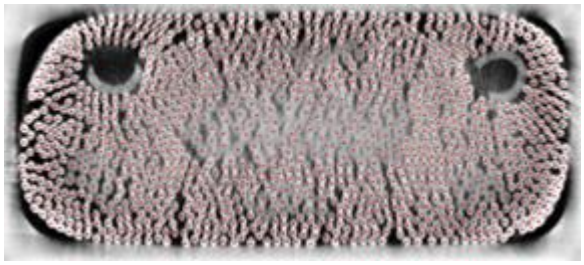

Fig. 3. Strands detection and positioning

We develop a simple algorithm that fits all the pixels inside a rectangular box, big enough to cast a strand section. The Gaussian profile parameters are measured on each pixel and if its values are greater than a given threshold, the strand's position is obtained and the box is slide in other position where the process is repeated and continued on all the slices. If multiple detections are obtained in the same box, an iterative process is done by increasing the threshold value, till a convergence is reached. Fig. 3 shows the centroids of the strands over-imposed on the tomographic cross-section. The rate of detection is strongly connected with image background noise. For the 400 kV scans a relatively good signal-to-noise ratio permits a rate of detection of over 99%.

Further on, when all the positions of the strands are detected on all the tomograms, one must connect the centroid of strands section from slice i to its correspondent section on slice i+1. This is done by fitting all the centroids from all the slices using a polynomial function or sum of sines of order n (in our case, we choose the order n=8). In Fig. 4 a) one shows the 3D plot of strand trajectories (only 20% are plotted from the total number of 1232 strands detected). In the same panel one shows a single strand with elliptically shaped cross-section as resulted by fitting the strands' pixels with a 2D Gaussian function. Thus one can retrieve the values from the contour that are right on the edge of the strand.

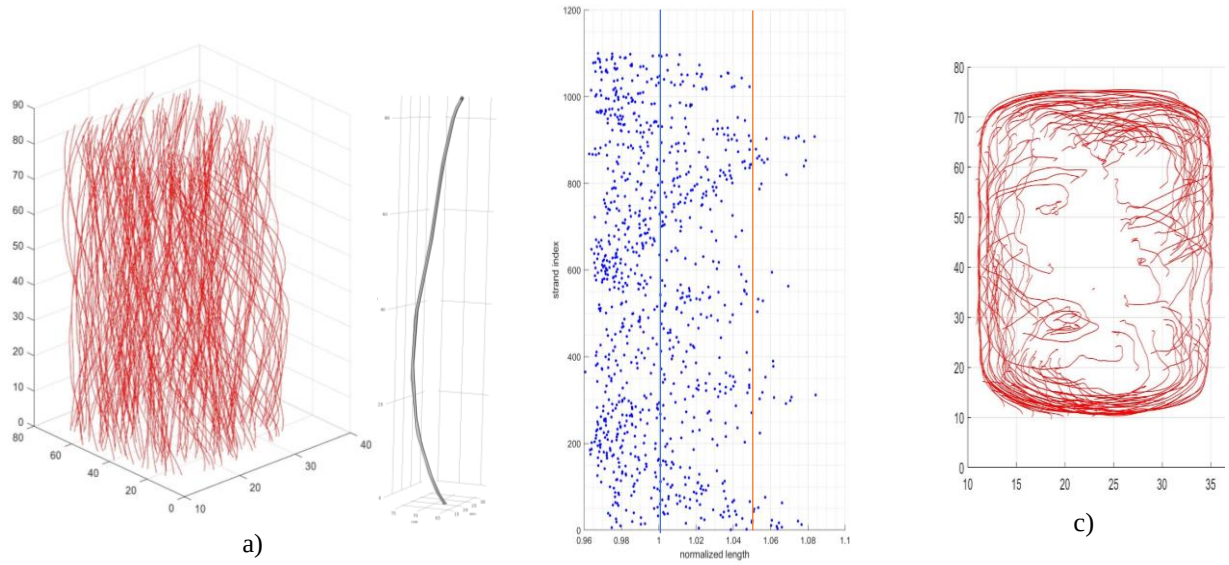

a) b) c)

Fig. 4. a) 3D representation of reconstructed strand trajectories (only 20 % of trajectories are represented) and a single strand with elliptically shaped cross-section; b) normalized strand length (average length -blue vertical line, lengths 5% longer than average – orange line) c) strands trajectories 5% longer than average projected on transversal plane.

An important engineering parameter of the CICC conductor is cos(θ) which represents the ratio of the conductor length to the average length of the strands. The input data for the calculation of cos(θ) parameter, i.e the reconstructed strand lengths, are plotted in Fig 4 b) while the plane projection of trajectories, 5% longer than the average, are represented in Fig 4 c). The cos(θ) for a sample of ~120 mm length is 0.96.

3.2 Strand level

Nb_3Sn strands with 19 tin centers of Western Superconducting Technology (WST) production are used for the fabrication of the ENEA DEMO prototype. The microtomography system was adjusted to deliver a stable, line pattern better than 1.5 µm on the JIMA Micro Resolution Chart for X-Ray. Thus, one generates volumetric images with spatial resolution almost similar in quality to an overview SEM. This image quality is sufficient for microstructural integrity assessment of the Nb_3Sn both before and after heat treatment as well as for a non-invasive evaluation of the twist-pitch factor.

Strand microstructure before and after heat treatment

Microtomography analysis of Nb_3Sn strands microstucture before and after heat treatment (Fig. 5 a, b) capture several features of interest as: structural integrity of Ta barrier, development of voids in the tin deposits and their consumption during the alloying phase, cracks formation and swelling of the Nb sleeves during the tin diffusion etc. Same type of analysis can be applied to strand samples after thermal/mechanical cycling.

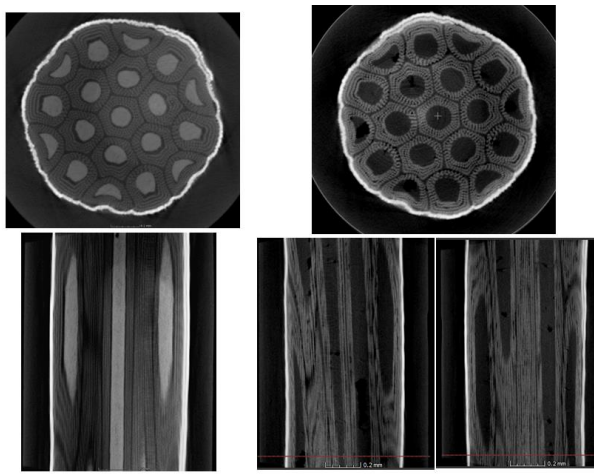

a) b)

Fig. 5. Comparison of Nb_3Sn strand microstructure by microtomography analysis a) before and b) after heat-treatment

Twist pitch factor

The twist pitch (TP) mainly influences the coupling loss of the conductor.

In [14] the authors present three methods, all of them of intrusive nature (repetition of filament bundles, angle of the filaments and rotation) for twist-pitch measurement and compare them. A non-invasive method based on the analysis of successive adjacent 3D microtomography scans of a strand sample is introduced in [9].

Here, we applied a procedure for twist-pitch evaluation based on image processing of multiple adjacent high resolution reconstructed volumes (Fig. 6). For each volume, the processing steps include: tomography image segmentation, contours detection and positioning of the tin centers and, finally, determination of rotation angle of the centroids projection on a transversal plane. For a 19 tin centers WST strand as used in the ENEA CICC cable a TP value of 14.5 ±0.8 mm was determined from seven

volumes scanned over 18 mm. This value is within the nominal specification (15±2 mm) of the manufacturer [14]..

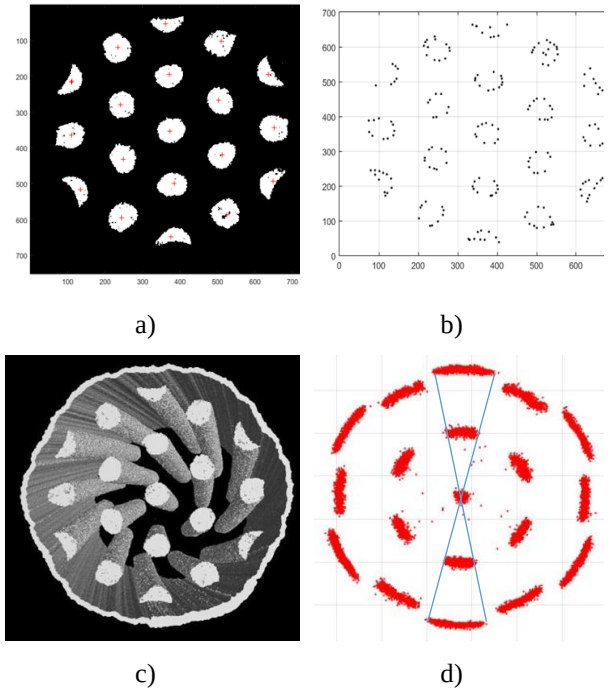

Fig. 6. Illustration of the procedure for twist-pitch evaluation using multiple high resolution reconstructed volumes. a) tomography image segmentation, b) tin deposits contours detection, c) 3D representation of tin deposits and Ta barrier and d) determination of rotation angle of tin deposit centroids on a plane projection.

Conclusions

The non-invasive XCT examination methodology developed in this paper is an adequate tool for investigating at strand and cable scale of selected samples of superconducting CICC during their manufacture and testing.

The accurate determination of the strand trajectories of relevant section of superconductor cables in 3-D coordinates format represents the key ingredient for obtaining an accurate 3D modeling of the CCIC cables.

Other parameters, such as local void fractions and cos(θ) are found in good agreement with the nominal values.

At strand level it is possible to evaluate in a non-invasive way the twist-pitch factor and also to compare the microstructures of the Nb_3Sn strands before and after heat treatment or mechanical tests.

The XCT environment established in this work is available for advanced NDT tasks for other conductors, including the newly developed HTS CICCs.

Acknowledgments

This work has been carried out within the framework of the EUROfusion Consortium and has received funding from the Euratom research and training programme 2014-2018 under grant agreement No 633053. The views and opinions expressed herein do not necessarily reflect those of the European Commission.

References

[1] Corato, V., et al. "Progress in the design of the superconducting magnets for the EU DEMO." Fusion Engineering and Design (2018).

[2] Bruzzone, Pierluigi, et al. "Design, manufacture and test of a 82 kA react&wind TF conductor for DEMO." IEEE Transactions on Applied Superconductivity 26.4 (2016): 1-5.

[3] Muzzi, Luigi, et al. "Design, manufacture, and test of an 80 kA-class Nb_3Sn cable-in-conduit conductor with rectangular geometry and distributed pressure relief channels." IEEE Transactions on Applied Superconductivity 27.4 (2017): 1-6.

[4] Uglietti, D., et al. "Progressing in cable-in-conduit for fusion magnets: from ITER to low cost, high performance DEMO." Superconductor Science and Technology 31.5 (2018): 055004..

[5] Bonifetto, Roberto, et al. "Thermal–hydraulic test and analysis of the ENEA TF conductor sample for the EU DEMO fusion reactor." IEEE Transactions on Applied Superconductivity 28.4 (2018): 1-9.

[6] Savoldi, L., et al. "Quench Propagation in a TF Coil of the EU DEMO." Fusion Science and Technology 72.3 (2017): 439-448.

[7] Tiseanu, Ion, et al. "Characterization of superconducting wires and cables by X-ray micro-tomography." Fusion Engineering and Design 88.9-10 (2013): 1613-1618.

[8] Hemmi, T., et al. "Investigation of Strand Bending in the He-Inlet During Reaction Heat Treatment for ITER TF Coils." IEEE Transactions on Applied Superconductivity 24.3 (2014): 1-4.

[9] Tiseanu, Ion, et al. "Accurate 3D modeling of cable in conduit conductor type superconductors by X-ray microtomography." Fusion Engineering and Design 98 (2015): 1176-1180.

[10] Tiseanu, Ion, et al. "3D X-ray micro-tomography for modeling of Nb_3Sn multifilamentary superconducting wires." Fusion Engineering and Design 82.5-14 (2007): 1447-1453;

[11] Badica, P., et al. "Microstructure of MgB2 samples observed by x-ray microtomography." Superconductor Science and Technology 21.11 (2008): 115017.

[12] Commisso, Maria S., et al. "Nondestructive Analysis of Nb_3Sn CICC and Strand by X-Ray Tomography." IEEE Transactions on Applied Superconductivity 26.3 (2016): 1-5.

[13] Scheuerlein, Christian, Marco Di Michiel, and Florin Buta. "Synchrotron radiation techniques for the characterization of Nb_3Sn superconductors." IEEE Trans. Appl. Supercond. 19.CERN-AT-2008-039 (2009): 2653-2656.

Haibel, A., Scheuerlein, C. Synchrotron Tomography for the Study of Void Formation in Internal Tin Nb_3Sn Superconductors. IEEE transactions on applied superconductivity, 17(1), (2007), 34-39.

[14] Fang, Liu, et al. "Comparison and analysis of twist pitch length test methods for ITER Nb_3Sn and NbTi strands." Rare Metal Materials and Engineering 44.9 (2015): 2095-2099.